



Dynamics of Particles Associated with Viral Infection of Marine Bacteria: Implications for Optical Variability

Julia Uitz^{1*}, Anne-Claire Baudoux^{2*}, Vanessa M. Wright¹, Francesca Malfatti², Jean Dubranna¹, Farooq Azam², Dariusz Stramski¹

Scripps Institution of Oceanography, ¹Marine Physical Laboratory, ²Marine Biology Research Division, University of California San Diego, La Jolla, CA 92093 USA (juitz@ucsd.edu)
*Both authors contributed equally to this work

1. Introduction

> **Context:** Particle size distribution (PSD) is a major determinant of seawater optical properties, yet the PSDs and optical properties are rarely measured concurrently. Historically, the PSD measurements have been usually focused on > 1 μm particles.

> **Objective:** To examine how the **optical properties respond to PSD dynamics** induced by viral infection of a marine bacterium - a case study.

> **Key feature:** **Concomitant measurements of optical properties and PSD** over a **broad size spectrum**, including **colloids** (roughly defined as < 1 μm particles), using a **combination of different instruments**.

> **Strategy:** Monitoring optical properties and PSD over a 3-day period following the infection of marine bacteria by specific bacteriophage.

2. Experiment Design

> **Host and phage cultures:** SWAT-3 host (marine γ-proteobacteria, *Vibrionales*) was inoculated in Zobell medium and grown overnight at room temperature in darkness. SWAT-3 phage was amplified by the plate lysis method using ultrafiltered autoclaved seawater as elution solution.

> **Procedure:** Pellets of host culture were resuspended in phage suspension and incubated 15min to allow phage adsorption; unadsorbed phages were removed by low-speed centrifugation; bacteria and adsorbed phages were resuspended in ultrafiltered seawater. Control of SWAT-3 host culture (no phage addition) was treated similarly. Infected and uninfected (control) samples were incubated at room temperature under gentle agitation in darkness. Samples were collected periodically during 72h incubation period.

3. Measurements

> **Optical properties:**

✓ $c_p(\lambda)$, $a_p(\lambda)$, and $b_p(\lambda) = c_p(\lambda) - a_p(\lambda)$ - Lambda-18 spectrophotometer (Perkin-Elmer) equipped with an integrating sphere using special geometric configurations for measurements in a 1 cm cuvette. Samples appropriately diluted to meet criteria of single scattering regime.

✓ Volume scattering function (VSF) at 18 angles (14.4°-163.3°) and $\lambda = 532$ nm - Dawn Eos (Wyatt Tech.). Vertically and horizontally polarized incident beam were used to estimate unpolarized VSF.

> **Particle size distribution:**

✓ Colloids (~20-500 nm) - Eclipse-Dawn Eos (Wyatt Tech.) system which combines Flow Field Flow Fractionation (FI FFF) and multi-angle light scattering measurement (vertically polarized light only); ultrafiltered seawater used as the carrier solution.

✓ 0.5-60 μm particles - Electrical resistive particle sizer Coulter Multisizer III (Beckman-Coulter) using 20 μm and 100 μm aperture tubes.

✓ Nominally 1-200 μm particles - LISST-100X Laser In Situ Scattering and Transmissometer (Sequoia Scientific) equipped with 532 nm laser.

> Viruses and bacteria counts - Epifluorescence microscopy (filters stained with Sybr Green I).

> Ultrafiltered seawater used as the diluent and blank for all measurements - Vivaflow 200 (Sartorius) equipped with a 10 kDa MWCO PES membrane.

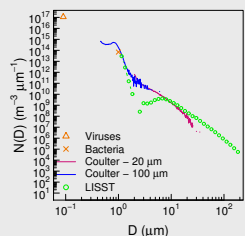


> **Fig. 1:** Example of density function of PSD for particle number concentration $N(D)$ vs. particle diameter D , measured using the Coulter and LISST instruments. Also shown are microscope counts of viruses and bacteria converted to $N(D)$, assuming a size range for these populations of 0.07-0.11 μm and 0.8-1.2 μm, respectively. A broad size range is covered by combining data from the two instruments. Additional analysis with FI FFF further extends the examined size range to include the colloidal particles (see Fig. 6).

4. Optical Properties

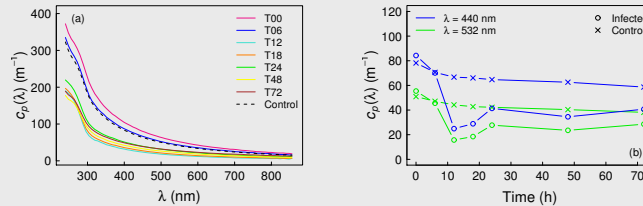


> **Fig. 2:** Beam attenuation coefficient, c_p . (a) Spectra for the infected sample at 7 sampling times; also shown is the mean for the control. (b) Time changes in $c_p(440)$ and $c_p(532)$ for the infected and control samples. ↪ 12h after infection we observe a 3.5-fold drop in c_p , which is associated with a decrease in bacterial abundance and the formation of colloids (see Figs. 6-7).

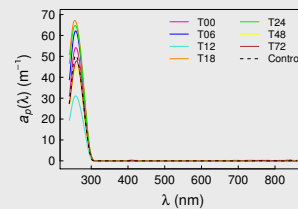


> **Fig. 3:** Spectral particulate absorption coefficient, a_p , for the infected sample at 7 sampling times; also shown is the mean for the control sample. ↪ Note that a_p is null at visible wavelengths so that, in this region, c_p equals to b_p . The strong absorption in the UV region is due to proteins and DNA from intact and lysed bacteria (cell debris).

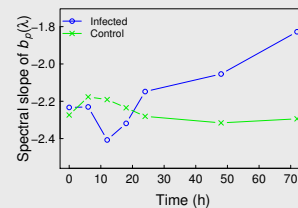


> **Fig. 4:** Time changes in the spectral slope of the scattering coefficient, $b_p(\lambda)$. Slopes were obtained from linear regression on log-log transformed data. The UV region was excluded from this analysis (due to the effect of anomalous dispersion of refractive index within the strong UV absorption band).

↪ Changes in b_p slope suggest (i) an increase in the relative contribution of small-sized particles 12h after infection, and (ii) an increase in the relative contribution of large particles throughout the rest of the experiment.

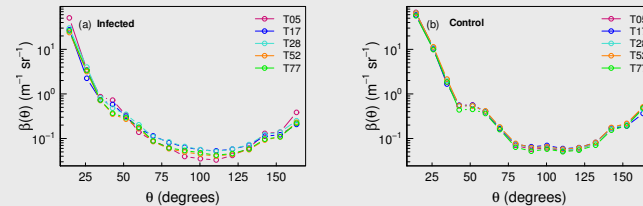


> **Fig. 5:** VSFs measured during the experiment for the infected and control samples. ↪ Variations in VSF over time display different behavior at different angles. The interpretation of these variations requires further investigation, for example using modeling approaches to light scattering with our input experimental PSD data.

5. Particle Size Distribution

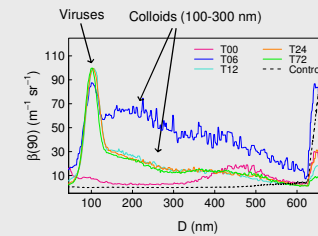


> **Fig. 6:** Fractograms (FI FFF) for infected sample at selected times and the mean curve for control. The particle diameter D is retrieved from calibration using standard nanospheres. ↪ The increase in viral abundance is accompanied by the formation of colloids within 6h after infection. After 6h, the abundance of colloids remains stable likely due to a balance between the sources (colloid production through lysis) and losses (transfer to the pool of large-sized particles through aggregation and/or formation of gels).

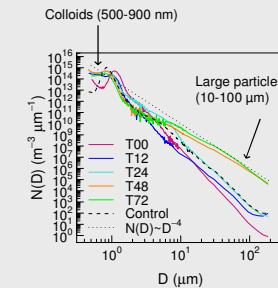


> **Fig. 7:** PSD reconstructed from the Coulter and LISST measurements for the infected sample at selected times and the mean curve for control. Dotted line represents the power law with a slope of -4 (often assumed for oceanic waters). ↪ Note the relative increase of large-sized particles (> 10 μm) with time throughout the experiment. As the slope of PSD varies with D , an idealized power function with a single slope is not appropriate for describing the PSD dynamics in our experiment.

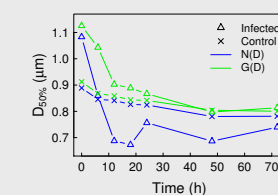


> **Fig. 8:** Time changes in the median diameter, $D_{50\%}$, calculated from the PSDs representing the particle number concentration, $N(D)$, and the particle projected-area concentration, $G(D)$. ↪ Within 12h, $D_{50\%}$ drops by about 35% using $N(D)$, or 20% using $G(D)$, from above 1 μm to below 1 μm. Note the similarity of temporal patterns of $D_{50\%}$ and c_p (cf. Fig. 2b).

6. Summary

> PSD dynamics associated with viral infection of bacteria on timescales from a few hours to a few days produce rapid and significant changes in optical properties.

> The PSD can be measured within a broad size spectrum using a combination of instruments based on different principles for particle sizing. Further work involving a combination of FI FFF with multi-angle light scattering is required to provide quantitative information about PSD in the colloidal size range ($D < 500$ nm).

> It is essential to advance measurement capabilities towards the acquisition of data on complete PSD spanning several orders of magnitude in particle size, including the small-sized colloids, to better understand variability in the inherent optical properties driven by particle dynamics.

> Dynamics and interactions between marine biological particles do not necessarily produce the PSD that follows the commonly assumed behavior of a power function with a single slope, which may have important implications to optical modeling.

